RESEARCH ARTICLE

Predicting anti-cancer drug combination responses with a temporal cell state network model

Deepraj Sarmah[1], **Wesley O. Meredith**[1], **Ian K. Weber**[1,2], **Madison R. Price**[1,3], **Marc R. Birtwistle**[1,4]*

1 Department of Chemical and Biomolecular Engineering, Clemson University, Clemson, South Carolina, United States of America, **2** The University of Virginia School of Medicine, Charlottesville, Virginia, United States of America, **3** College of Pharmacy, Medical University of South Carolina, Charleston, South Carolina, United States of America, **4** Department of Bioengineering, Clemson University, Clemson, South Carolina, United States of America

* mbirtwi@clemson.edu

Abstract

Cancer chemotherapy combines multiple drugs, but predicting the effects of drug combinations on cancer cell proliferation remains challenging, even for simple *in vitro* systems. We hypothesized that by combining knowledge of single drug dose responses and cell state transition network dynamics, we could predict how a population of cancer cells will respond to drug combinations. We tested this hypothesis here using three targeted inhibitors of different cell cycle states in two different cell lines *in vitro*. We formulated a Markov model to capture temporal cell state transitions between different cell cycle phases, with single drug data constraining how drug doses affect transition rates. This model was able to predict the landscape of all three different pairwise drug combinations across all dose ranges for both cell lines with no additional data. While further application to different cell lines, more drugs, additional cell state networks, and more complex co-culture or *in vivo* systems remain, this work demonstrates how currently available or attainable information could be sufficient for prediction of drug combination response for single cell lines *in vitro*.

Author summary

Cancer chemotherapy combines multiple drugs, but determining which drugs would be efficacious for particular patients remains extremely challenging. Experimental solutions to this problem are not yet possible due to the large space of possible combinations of hundreds of anti-cancer drugs. Computational models may help, but it is not yet clear how such models should be built and what elements they need to capture to predict drug combination response. In this work, we explored the idea that if we knew something about the proportions of different types of cancer cells in a population, how fast transitions happen between the different types, and how individual drugs affect those transitions, that we might be able to build a computational model that predicts drug combination responses based only on feasible single drug response experiments. We

tested this idea using simple cell culture systems with two different cancer cell lines and three different anti-cancer drugs, and found surprisingly good agreement between computational model predictions and experimentally measured drug combination responses. While further application to different cell lines, more drugs, and more complex experimental systems remain, this work demonstrates how currently available or attainable information could be sufficient for prediction of drug combination responses.

Introduction

Matching chemotherapy regimens to cancer patients remains a grand challenge of oncology and personalized medicine. Targeted drugs often have genetic biomarkers, such as BRAFV600E for vemurafenib [1,2], EGFR mutations and copy number amplification for gefitinib [3–5], BCR-ABL fusion for imatinib [6,7], and HER2 copy number amplification for trastuzumab [8,9]. However, such matched patients often do not respond to therapy and/or eventually develop resistance. Why? One major driver is tumor heterogeneity; cells in different "states" that have different drug sensitivities. Genomic status (and mutational heterogeneity across a population)[10] is one dimension of cell state, but cell states are also defined by their histology or transcriptomics (through for example single cell RNAseq experiments) [11–17], and it is becoming appreciated that cells can transition between such states in development-like networks, sometimes called cell state networks [13,18]. Such plasticity between cell states can contribute to drug resistance [19–21], and combinations of drugs targeting different pathways and factors involving phenotype transition have been proposed to prevent such resistance [19]. Another is the multi-variate complexity of biochemical networks within which drug targets reside and by which chemotherapy drugs exert their action [22–27]. These networks can differ between cell states, adapt to therapy, and also give rise to non-intuitive therapy results, such as feedback loops and compensatory pathways underlying the efficacy of combining Raf and MEK inhibitor combinations, which lie in the same genetic pathway [28–31].

Massive agnostic efforts have screened thousands of cancer cell lines for sensitivity to hundreds of anti-cancer drugs, with matched multi-omic data to mine for biomarkers predictive of drug response [32–39]. These efforts, while substantial, still have not solved the problem of how to match patients to drugs. Moreover, many chemotherapy regimens comprise combinations of 3–4 drugs. Comprehensive experimental exploration of just 2-way drug combinations for hundreds of anti-cancer drugs across a representative cohort is infeasible clinically, and currently unreachable even in cell culture systems.

The inability to obtain an experimental solution to the problem of matching drug combinations to patients has motivated computational modeling approaches. In principle, more comprehensive exploration of drug combination space could be achieved *in silico*. Various computational methods including mechanistic models and machine learning approaches have shown promise in predicting drug combination responses, especially taking into consideration context specific pathology and omics data as well as identifying specific biomarkers and drug-targets [40–45]. Regardless of the modeling methods being used, there is a widespread focus on using information about biochemical networks to facilitate drug combination response prediction [27,46–48]. Despite advanced methods being applied to integrate such information into models, building predictive drug combination response models remains an unsolved challenge. Any solution to this problem must invariably rely on experimental data that is already existing or is realistically attainable, such as single drug dose responses.

In this paper, rather than focus on modeling biochemical networks, we test the hypothesis that by combining knowledge of single drug dose responses and cell state transition network

dynamics, we could predict how a population of cancer cells will respond to drug combinations. Although this hypothesis runs contrary to the predominant biochemical network-centered view of this problem, cell state transitions are largely governed by biochemical networks in which drug targets are embedded, so in a sense this idea is encompassing prior logic. We test this hypothesis by focusing on three drugs that target cell cycle transitions in two different cell lines *in vitro*. A Markov model is developed to capture population growth dynamics and single drug dose responses, and then this model is used to predict all two-way drug combination responses with no further adjustment. Comparison of these model predictions to experimental tests shows surprisingly good agreement, despite the simplicity of the model. These results suggest a sufficient formulation for predicting how single cell line population growth dynamics *in vitro* respond to drug combinations, relying only on currently available and/or attainable information. If this idea scales upon more extensive testing with additional cell lines, drugs, and more complex biological scenarios such as co-culture or *in vivo* systems it could have widespread impact on precision oncology efforts.

Results

To test our hypothesis that knowledge of single drug dose responses combined with cell state transition network dynamics could enable prediction of drug combination responses (**Fig 1A**), a model system is needed. There are a variety of choices for cell state transition networks and drugs which modulate them; here we focus on the cell cycle and three targeted kinase inhibitors (**Fig 1B**). Specifically, we focus on a MEK1/2 inhibitor (PD0325901) that primarily blocks transition of G_0/G_1 cells [49], a CDK4/6 inhibitor (abemaciclib) that primarily blocks transition of (late)G_1/S cells [50–53], and a PLK1 inhibitor (TAK-960) that primarily blocks transition of G_2/M cells [54–57]. Drug dose response experiments evaluating cell number after 3 days of treatment show that both U87 and U251 cells are responsive to these drugs as single agents (**Fig 1D**). These cell lines and drugs were chosen as a subset of a larger ongoing project; however, the hypothesis under investigation is agnostic to the particular cell lines and drugs chosen. Wider application beyond this initial set would enable more extensive evaluation of how substantial differences between cell lines and drugs impact the hypothesis.

Before accounting for drug effects, we first constructed and parameterized a temporal cell state network model based on Markov formalisms that describes cell population growth dynamics in the absence of drug for U87 and U251 cells. The reader is referred to the Methods section for full details of model assumptions, development, and parameter estimation. Cells in the G_0/G_1 state can transition to the (late)G_1/S state, which can then transition to the G_2/M state. Upon transition from G_2/M to G_0/G_1, cell division occurs, increasing cell number by one. For this case without drug, we consider cell death transitions (which decrease cell number by one) to be negligible. In each time step (chosen to be 1 hr), cells can either remain in their current state, or transition. We estimated the three unknown transition probabilities for each cell line by requiring agreement with population doubling time (31.13 hours-U87 [58–60] and 24.93 hours-U251 [61–63] and the steady-state cell state ratios (60:24:16 for U87 [64–68] and 58:23:19 for U251 [69–71]) (**Fig 1C and Table 1**). Simulations recapitulate these features. There is variability reported in the literature for the doubling time and steady-state cell state ratios; below we evaluate the effects of this variability on drug combination response predictions.

Drug action was modeled by assuming the transition probabilities are a sigmoidal function of drug dose (see Methods). Biologically, we assume that PD0325901 blocks transition of G_0/G_1 cells [49], Abemaciclib blocks transition of (late)G_1/S cells [50–53], and TAK-960 blocks transition of G_2/M cells [54–57]. Fitting to the single drug dose response data yielded
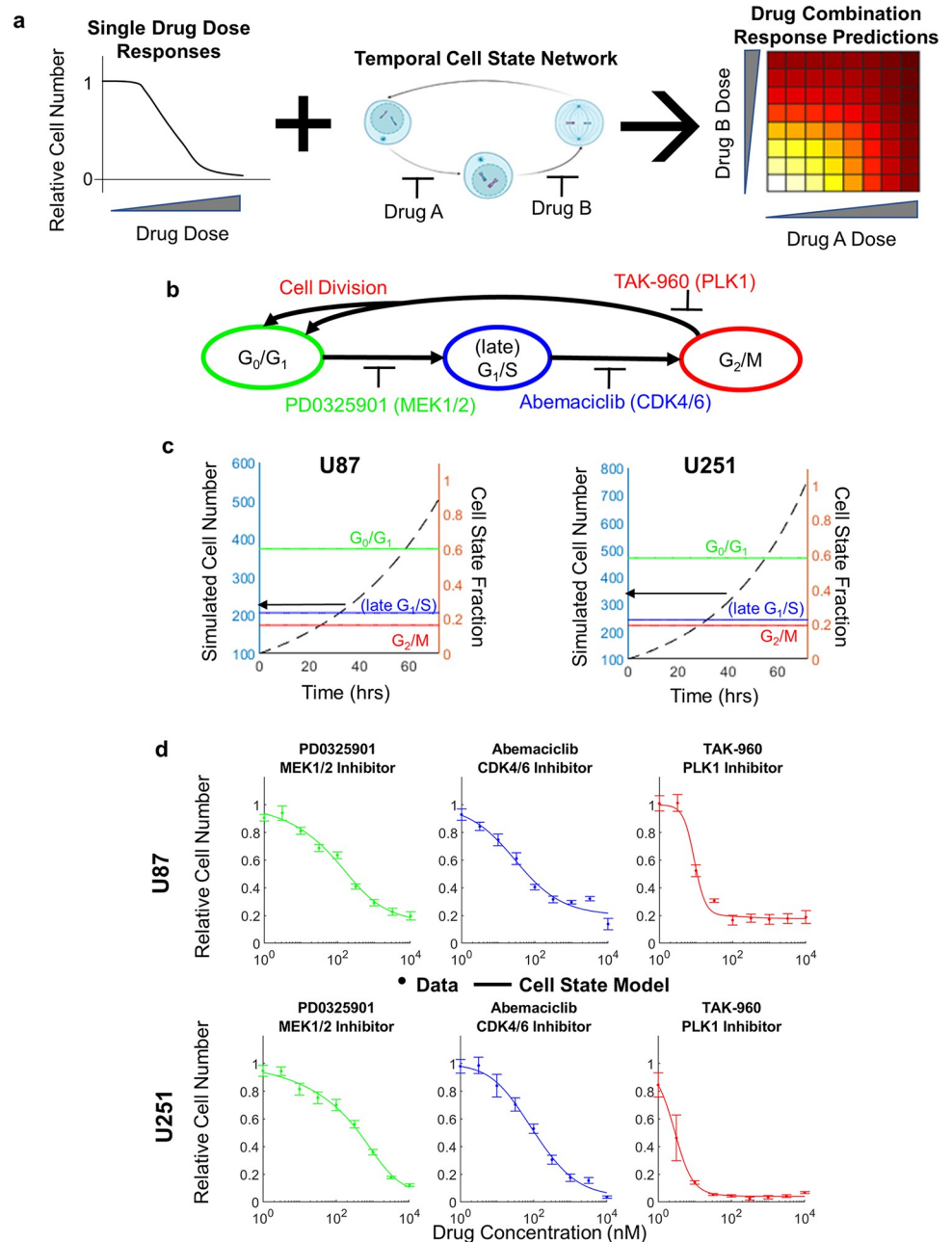
Fig 1. Modeling temporal cell states and single drug dose responses. (a) Graphical abstract. Schematic showing the idea that integration of single drug dose response experiments with temporal cell state network models might enable prediction of drug combination responses. **(b)** Schematic of the temporal cell state network comprising G0/G1, late G1/S and G2/M states and the activity of the drugs PD0325901, Abemaciclib and TAK-960 in each state. In this work, we assume that the action of each drug is specific to the state indicated by color. Cells exiting G2/M divide when they re-enter G0/G1. **(c)** Time courses of cell number in the temporal cell state model for U87 and U251 cells starting with 100 cells for 72 hours. Cell proportions at G0/G1, late G1/S and G2/M states are also shown, which remain constant. **(d)** Single drug dose responses for PD0325901, Abemaciclib and TAK-960 in U87 and U251 cells at 72 hours (points) compared to model predictions (lines). Error bars denote standard error.

reasonable agreement between model and data for most drug doses, but with some systematic variation at high drug doses (**Fig A in S1 Text**). The reason for this systematic variation was that cell counts for high drug doses were lower than the initial cell count, implying cell death

Table 1. Best Fit Markov Transition Parameters.

	U87	U251
$M_1\ (hr^{-1})$	0.05	0.07
$M_2\ (hr^{-1})$	0.11	0.15
$M_3\ (hr^{-1})$	0.14	0.15

https://doi.org/10.1371/journal.pcbi.1011082.t001

occurred. Therefore, we allowed the drugs to induce cell death (see Methods). This refined model could account for responses at high drug doses with improved agreement overall (r~0.99, ΔAIC = -160.1, **Fig 1D and B in S1 Text**). Overall, these results demonstrate that the Markov model of cell state transition dynamics can capture cell population growth and single drug responses for the investigated system.

Now that we had a model that could take as input any of the three drugs at any dose and simulate cell population dynamics, we could predict how drug combinations would affect cell number for all pairwise combinations of the three drugs (**Fig 2, left**). These predictions demonstrate reasonable agreement with independent experimental data for every drug combination for each cell line (r~0.92–0.99; **Fig 2-middle and right**). The largest discrepancies were evident for TAK-960, particularly for U251 cells (**Fig 2-bottom two rows**). These discrepancies seem to be predominantly due to experiment showing decreased sensitivity to TAK-960 as a single agent relative to the model (lighter color further to the right). This may be a result of (i) the steep dose response of these cells to TAK-960 ($n>1$, **Table 2**) combined with (ii) finer dose ranges used in the combination experiments around the responsive ranges (see Methods and Fig 2 legend), leading to greater uncertainty in these dose ranges based only on the single drug responses. Notably, no modifications were made to the model—only information about the cell state transition network dynamics and single drug dose responses were needed to perform this prediction. We evaluated the ability of the model to account for drug combination response data when the input doubling time and cell state ratio data were varied between maximum and minimum reported values (**Fig C in S1 Text**). The agreement between model and data was robust to this variation (r~0.92–0.99, similar to previous).

Analysis of drug combination responses often includes assessment of drug synergy or antagonism, a more qualitative and categorical analysis. A common analysis is excess over Bliss (EOB) [72], which captures how much of the observed drug response is beyond statistically independent action by each drug. In particular, we used a variation of excess over Bliss that is more robust and reproducible because it uses sigmoidal fits to data to mitigate the impact of experimental noise in any single data point [73]. Values close to zero indicate non-interacting combinations, positive values indicate synergistic combinations and negative values indicate antagonistic combinations. We calculated EOB for model and experiment, yielding an averaged single score for each drug combination / cell line pair, and evaluated agreement between the two (**Fig 3**). Both model and experiment show drug combinations were predominantly mildly antagonistic or non-interacting with co-localization in the bottom left quadrant. Overall, these results provide support for the hypothesis that responses to anti-cancer drug combinations can be predicted with a model of cell state transition dynamics and knowledge of single drug dose responses, for single cell lines *in vitro*.

Discussion

Predicting how varied drug combinations control cancer cell population growth is key to improving cancer precision medicine. Experimental solutions alone cannot cover the vast combinatoric space comprising drug combinations and different cancer cell types,
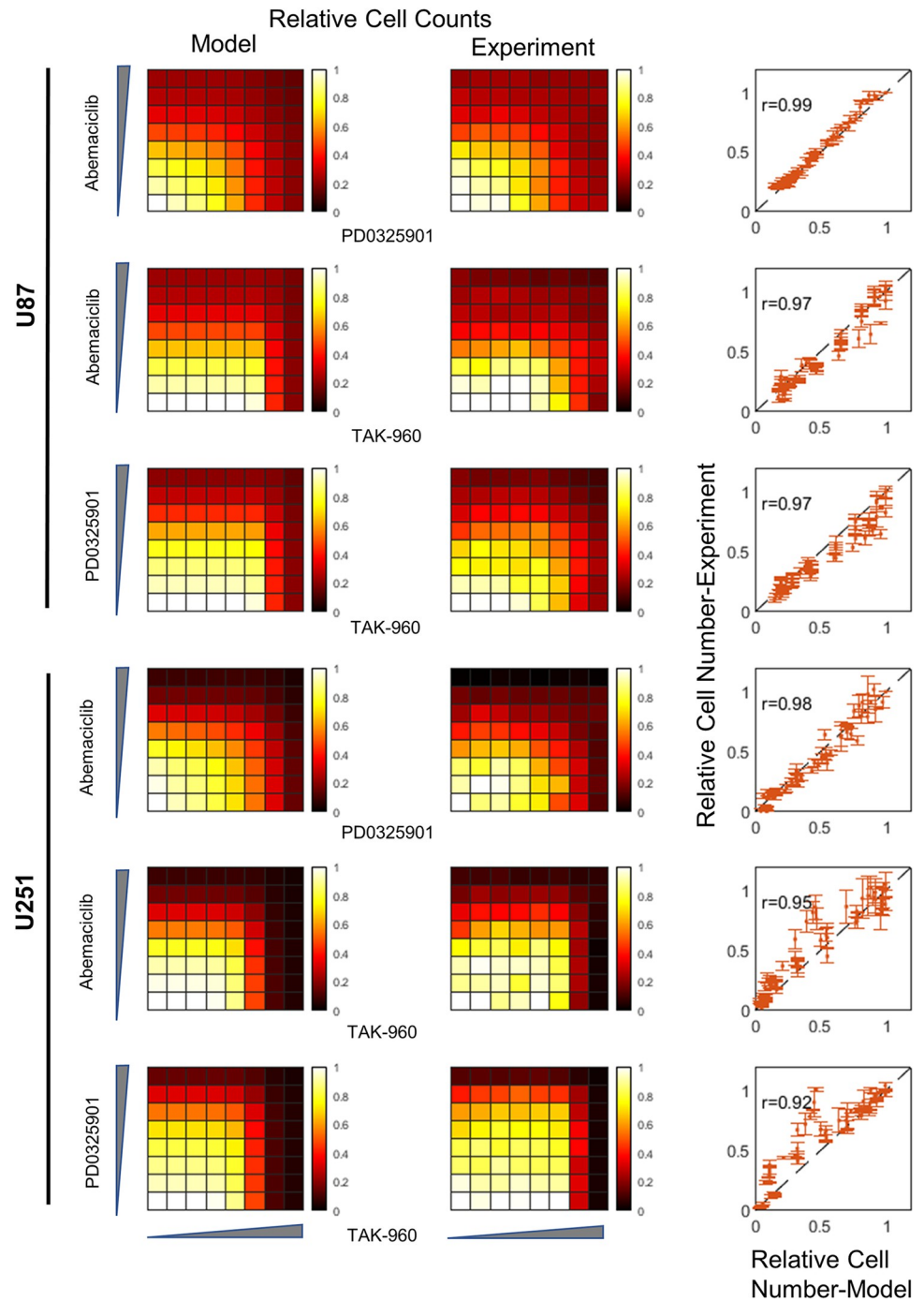
Fig 2. Model prediction vs experiments for drug combination responses. Predicted and measured combination drug dose responses for Abemaciclib/PD0325901, Abemaciclib/TAK-960 and PD0325901/TAK-960 for U87 cells (top) and U251 cells (bottom). First column is relative cell counts for model simulations, second column is relative cell counts for experiments, and the third column is a scatterplot for model vs experiment for relative cell counts. The drug concentrations (nM) for Abemaciclib and PD0325901 are 0, 1.22, 4.88, 19.53, 78.13, 312.5, 1250, and 5000, and for TAK-960 are 0, 0.012, 0.049, 0.20, 0.78, 3.13, 12.5, and 50. The correlation coefficient for agreement between model and experiment for each cell line/drug combination pair is indicated. Error bars denote standard error.

https://doi.org/10.1371/journal.pcbi.1011082.g002

Table 2. Best Fit Drug Response Parameters.

	PD0325901	Abemaciclib	TAK-960
U87			
EC_{50} (μM)	0.10	0.01	0.0073
n	0.50	0.65	2.88
$E_{max,\varphi}$ (hr^{-1})	0.011	0.0028	0.0025
$EC_{50,\varphi}$ (μM)	0.40	0.033	0.28
U251			
EC_{50} (μM)	0.56	0.19	0.0025
n	0.40	0.76	1.69
$E_{max,\varphi}$ (hr^{-1})	0.034	0.026	0.022
$EC_{50,\varphi}$ (μM)	2.77	0.042	0.0070

https://doi.org/10.1371/journal.pcbi.1011082.t002

necessitating computational approaches. Any computational approach should rely only on data that is available and/or feasibly attainable. Here, we explore the use of a computational approach that, rather than focus on biochemical networks in which drug targets reside, focuses on cell state networks where drugs influence transitions. By combining information about the cell state network dynamics with single cell drug dose responses, we were able to predict combination responses for three different targeted anti-cancer drugs in two different cell lines with no additional model modifications, with reasonable agreement between model and experiment ($r\sim0.92$–0.99). We expect this finding to be impactful to inform expansion to different drugs, cell types, and more complex biological systems such as co-culture or *in vivo* models.

The drugs studied here were found to be mildly antagonistic and have not been evaluated as combinations in other studies to our knowledge, including large-scale screening studies [38,74,75]. Interestingly, these previous large-scale screening studies suggest most drug combinations are non-interacting or antagonistic. The fact that the particular drugs studied were found to be antagonistic could be interpreted as a consequence of sequential action on

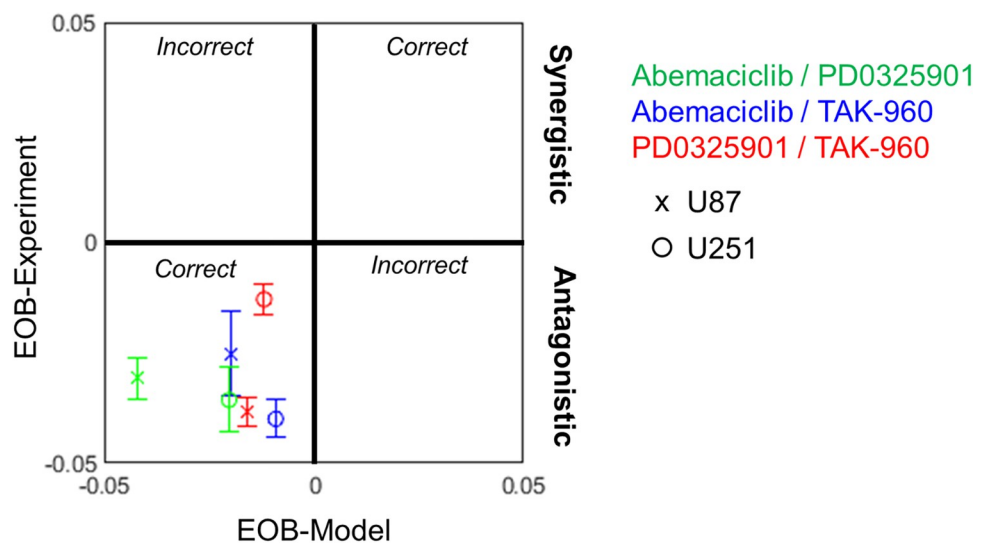**Fig 3. Excess Over Bliss Analysis.** Excess over Bliss (EOB) for each drug combination dataset in simulations and experiments were calculated as described in Methods, and mean summarized to obtain as single EOB score for each cell line / drug combination pair. Positive scores denote synergy while negative scores denote antagonism. Error bars are standard error.

https://doi.org/10.1371/journal.pcbi.1011082.g003

different cell cycle stages, with treatment of one stage resulting in fewer cells available to respond to other drugs, similar to a classical interpretation of negative cooperativity. Yet, a general theory for understanding how cell state or drug target network structure gives rise to drug combination behavior is not yet established, and future studies on this topic would be beneficial.

Combination therapy for the analogous drug targets of MEK1/2, CDK4/6, and PLK1 have been reported but paint an incomplete and inconsistent picture, which may be due to the lack of consistent experimental and analytical systems for evaluating synergy, as well as the large variation between different tumor and cancer cell line types. In KRAS mutant colorectal cancer, combinations of CDK4/6 and MEK inhibitors have been found to be synergistic in reducing *in vitro* cell growth, and to be effective in patient-derived xenograft models [76]. They were reported to cooperate in pancreatic cancer models as well [77]. The rationale was that resistance to the MEK inhibitor by reactivating the pathway could be blunted by also blocking downstream with the CDK4/6 inhibitor, similar to combined BRAF and MEK inhibition in melanoma [28]. Similarly, multiple cancers that had become resistant to CDK4/6 inhibition were found to be sensitized to MEK inhibition [78]. In a single NRAS mutant melanoma patient, this combination was found to be effective, perhaps related to CDKN2A mutation status [79]. A PLK inhibitor showed synergy with only one of two BRAF (upstream of MEK) inhibitors studied in a panel of melanoma cell lines [80], and demonstrated efficacy in a NRAS mutant melanoma [81]. PLK inhibitors were shown to be effective in ER-positive breast cancers that were resistant to CDK4/6 inhibition [82], however other studies showed antagonism in pancreatic cancer [77].

While this study provided support for the idea that drug combination response could be predicted from knowledge only of cell state networks and single drug dose response, it was limited to single cell lines *in vitro*, and only to three drugs and two cell lines. An obvious next step is scaling tests to more single cell lines and drugs. We expect that such scaling would reveal more difficult scenarios where a single drug may target multiple cell state transitions, or where multiple drugs may target the same cell state transition. New methodology would be needed to specify and constrain such mapping; mechanistic modeling of drug target networks could be of use here [22–26,38,41,83].

A single cell line *in vitro* is an extremely simple situation that neglects the impact of, for example, multiple non-tumor cell types, different tumor cell subclones, 3D environments, non-exponential (e.g. Gompertz-like) growth, and long-term development of drug resistance. More cell fates such as apoptosis (and variants such as ferroptosis and necroptosis), senescence, and movement should be considered. The model employed here also does not consider spatial phenomena that could influence cell-cell communication, both physical and chemical. The presence of multiple subclones and non-cancer cell types within a tumor could create cell populations and niches with different drug or immune sensitivities. Multiple agent-based modeling approaches have been described that are suitable for capturing these important phenomena [84–88]. Evolutionary dynamics on larger time scales are critical to capturing resistance, a major focus of combination therapy. Ecological and game theory models have been proposed to describe such effects, by proposing "adaptive therapy" regimens that intelligently (and in a sense optimally) switch between drugs to maintain tumor burden at manageable levels [89–93]. These types of models seem in principle compatible with the models and ideas described in this paper.

Pharmacokinetics are another important aspect that remains to be explored. Drugs are often given in different temporal sequences but here we only investigated simultaneous administration. The proposed cell state network models do have the ability to explore drug temporal sequence, and this is straightforward to implement with *in vitro* experiments, so this is a logical

next step for exploring how to better administer drug combinations. For eventual *in vivo* situations, drug concentration is not constant, but again, the dynamic nature of the cell state models is amenable to handling such changes. Lastly, drug concentration is not constant across spatial dimensions of the tumor. Integration with existing partial differential equation or agent-based models could help account for spatially-varying drug concentration [84–88].

While we do not explicitly consider the role of biochemical networks in drug combination response, in a sense, they are implicitly accounted for in the mapping of drug concentration to cell state transition rates. In the investigated case, there was an arguably clean mapping of drug concentration to single transition rates, which simplified the effort. In other cases, such mapping may not be known *a priori* and/or more complex, i.e., a single drug may influence multiple transition rates, or two drugs may impact the same transition rate. Biochemical network models that capture such complexities or mapping may prove useful in such situations [22–26,38,41,83]. Assumptions regarding the additivity (or not) of multi-drug action on transition probabilities would have to be asserted. The current availability of drug combination response data sets [74,75,94,95] could facilitate the testing of such methods. Such future work could explore drug combination features we did not consider here, such as combining drugs that are not effective as single agents. They could also explore conditions that lead to drug combination synergy; the systems chosen here exhibited predominantly antagonistic behavior. Avoiding antagonism, however, is likely an important goal. It is thought that a small fraction of all drug combinations lead to synergistic behavior [38,74,75], but finding them, and how synergy is controlled by cell type, is of critical importance for precision oncology.

Application of this approach to other systems requires identification of cell state network models. Again, in our case the cell cycle is well established in terms of cell state network structure, but other such networks may not be. For example, gliomas are thought to comprise a network of four fundamental subtypes that can transition between each other, and whose differential growth and drug response characteristics are important for predicting response to therapy [96]. Studies have also confirmed the factors behind certain other cell state transitions- for instance, the transcriptomic factors and signaling molecules in different epithelial to mesenchymal transitions [26,97–99]. Cell state transition networks have been identified for multiple cancer types [11–15,17,18,100–102], generally by combining single cell measurements (e.g. single cell RNAseq), with perturbation time courses, such as enriching for one cell state and then observing the fractional composition dynamics. Recently, we proposed a general theory built upon modular response analysis [103–106] that allows one to reconstruct cell state networks from such perturbation time course data [107]. This theory is compatible with the Markov formalisms used here. Such Markov formulation may have further applicability to other cell state systems [18,101,102,108–110], but other approaches have been used [111–114]. Cell state transitions are subject to inherent stochasticity and describing the cell transitions as a Markov process is a common tool to capture this probabilistic aspect. However, this also relies on the assumption that the transition probabilities and the underlying variables are known and that the cell states are properly sampled and well classified. There could be several knowledge gaps in these assumptions including that cells may be transcriptomically intermediate between canonically defined states [115] and biological data may be sparse [116]. Inclusion of methods such as lineage tracing and methods able to handle sparse data [113] may help address some of these gaps.

Overall, we have tested a relatively simple hypothesis that knowledge of single drug dose responses combined with cell state network dynamics is sufficient for prediction of drug combination responses. This hypothesis seems to hold true at least for the three drugs and two cell lines tested here *in vitro*, providing a potentially powerful rationale for guiding drug combination response modeling efforts. Expansion to more cell lines, cell state systems, and drugs will

of course be important for further testing. Our findings here provide an important step towards being able to predict how cancer cell populations will respond to combinations of anti-cancer drugs, a key capability for cancer precision medicine.

Methods

Experimental Methods

Cell culture.   U87 and U251 cells (both STR verified) were cultured in full growth medium comprising DMEM (Gibco #10313039) supplemented with 10% FBS (Corning #35-011-CV) and 2 mM L-Glutamine (Corning #25–005-CI). The cells were cultured at 37˚C in 5% CO_2 in a humidified incubator and passaged every 2–3 days with 0.05% trypsin (Corning #25–052-Cl) to maintain sub-confluency.

Single drug dose response experiments.   U87 and U251 cells were seeded in 96 well plates (Corning-Falcon #353072) with 500 cells per well, counted with a hemocytometer. Cells were seeded in 90 µl full growth media and cultured overnight. The next day, 10 µl of media containing 10X the final drug concentration was added and the plates cultured for 72 hours. Experiments were done in biological duplicate with technical triplicates for each.

The three drugs were procured from the following sources—PD0325901 (Selleckchem #S1036), Abemaciclib (Selleckchem #S5716) and TAK-960 (Tocris #5403). The quantities of each drug-PD0325901 (25 mg, molar mass-482.19g), Abemaciclib (25 mg, molar mass-506.59g) and TAK960 (10 mg, molar mass-598.06g) corresponded to 0.0518 millimoles, 0.0493 millimoles and 0.0167 millimoles respectively and were diluted in 5.18 mls, 4.18 mls and 1.67 mls of sterile filtered DMSO to bring the final concentration to 10 mM for each drug. These dilutions were then aliquoted into 10 µL batches. Before adding to cells, 990µL of full growth media was added to a 10 µL drug aliquot, diluting it to 100 µM, 10X times the highest desired dose. This concentration was further serially diluted 8 more times in full growth media containing 1% DMSO (to maintain the same DMSO concentration in each dilution) and by a factor of 3.16 each time. This results in 9 dilutions with the drug concentrations between 10 nM-100 µM. In 9 wells with cells seeded overnight in 90 µL media, 10 µL of the serially diluted drugs are added. In the 10th well, 10 ul of full growth media containing 1% DMSO was added as the vehicle control dose.

Drug combination response experiments.   U87 and U251 cells were seeded in 96 well plates (Corning-Falcon #353072) with 500 cells in each well. Eight by eight wells were seeded in 150 µl full growth media and cultured overnight. The next day, 25 µl of media was added twice to each well, each containing 8x of the final drug concentration and cultured for 72 hours. The final drug concentrations were chosen to reflect their responsive range for the cell lines (1.22 nM-5µM for PD0325901 and Abemaciclib, 0.0122nM-50nM for TAK960, with a factor of 4 spacing). Before adding the drugs to cells, as above, full growth media was added to a 10 µL drug aliquot, diluting it to 8X times the highest desired dose. This concentration was further serially diluted 6 more times in full growth media containing 1% DMSO (to maintain the same DMSO concentration in each dilution) and by a factor of 4 each time. Experiments were done in biological triplicate.

Staining and computational image analysis.   After 72 hours of treatment with the drugs, the cells were stained with Hoechst (BDBiosciences #BD 561908) and Propidium Iodide (Millipore Sigma #P4170) at a final concentration of 1 µg/ml and 2 µg/ml to stain all cells and dead cells, respectively. After 30 minutes, the wells were imaged using the TagBFP (Excitation-390/18 nm, Emission-447/60 nm) and RFP filters (Excitation-531/40 nm, Emission-593/40 nm) in a Cytation 5 (Biotek). Each image was flatfield corrected and background subtracted using CellProfiler. The nuclei were then identified using the `IdentifyPrimaryObjects` feature, and a pseudo image was generated. The number of all counts of cell nuclei stained

with Hoechst and Propidium Iodide were compiled by CellProfiler and exported as csv files (provided in the code). The Propidium Iodide-stained nuclei counts were subtracted from the Hoechst stained nuclei counts for each well, and this was taken as the live cell counts which were the primary data.

Computational methods

Biological assumptions.   We assume that cells in the G_0/G_1 state can transition to the (late)G_1/S state, which can then transition to the G_2/M state. Upon transition from G_2/M to G_0/G_1, cell division occurs, increasing cell number by one. Without drug, we consider cell death transitions (which decrease cell number by one) to be negligible. In each time step (chosen to be 1 hr), cells can either remain in their current state, or transition. Drug action was modeled by assuming the transition probabilities are a sigmoidal function of drug dose (see below). PD0325901 blocks transition of G_0/G_1 cells [49], Abemaciclib blocks transition of (late)G_1/S cells [50–53], and TAK-960 blocks transition of G_2/M cells [54–57]. We allow for each drug to also induce cell death since a model without this could not account for data at high drug dose (**Fig A in S1 Text**).

Markov model of temporal cell state transitions.   Consider a Markov transition model comprising three nodes, representing cell states G_0/G_1, late G_1/S and G_2/M, denoted 1, 2, and 3 in short. M_1, M_2 and M_3 are the proportions of cells transitioning from states 1–2, 2–3 and 3–1 respectively, within a given timestep, taken to be one hour. M_{11}, M_{22} and M_{33} are the proportion of cells that do not transition from states 1, 2 and 3 respectively, in that hour. A cell in state 3 undergoes cell division which gives rise to two cells in state 1. We formulate this scenario using a jump Markov process model as follows:

$$x_{1,t+1} = M_{11}x_{1,t} + 2 \times M_3 x_{3,t}$$

$$x_{2,t+1} = M_{22}x_{2,t} + M_1 x_{1,t}$$

$$x_{3,t+1} = M_{33}x_{3,t} + M_2 x_{2,t} \qquad (1)$$

where, $x_{i,t}$, are the numbers of cells in state i at time point t. We set the time interval between two Markov jumps at 1 hour and simulate the model for a total of 72 hours.

These equations are subject to the constraints that the proportion of cells within a state must add to 1. Therefore,

$$M_{ii} + M_i = 1 \qquad (2)$$

or

$$M_{ii} = 1 - M_i \qquad (3)$$

Incorporating this in the above equation enables representation of the system in terms of M_1, M_2 and M_3 only:

$$x_{1,t+1} = (1 - M_1)x_{1,t} + 2 \times M_3 x_{3,t}$$

$$x_{2,t+1} = (1 - M_2)x_{2,t} + M_1 x_{1,t}$$

$$x_{3,t+1} = (1 - M_3)x_{3,t} + M_2 x_{2,t} \qquad (4)$$

In short this may be represented as follows

$$x_{i,t+1} = (1 - M_i)x_{i,t} + f \times M_j x_{j,t}$$

$$if \; i = 1 : f = 2, j = 3$$

$$if \; i = 2,3 : f = 1, j = i - 1 \tag{5}$$

We estimated the unknown transition rate parameters M_1, M_2, and M_3 based on experimental data for cell doubling times of 31.13 and 24.93 hours and cell state ratios (G0/G1:G1/S:G2/M) of 0.602:0.235:0.163 and 0.581:0.225:0.194 for U87 and U251 cells respectively (data references in Results). For U87, max/min values were 37.1/25.5 and 0.668:0.263:0.069 / 0.54:0.23:0.23. For U251 max/min values were 27.8/23.0 and 0.716:0.204:0.08 / 0.482:0.237:0.281 (Fig C in S1 Text). We used the doubling time (τ_d) to estimate how many cells should be present after 72 hours starting from 100 cells ($100e^{72*ln(2)/\tau_d}$), and multiplied this number by the cell state ratios to estimate $x_{1,72}$, $x_{2,72}$, and $x_{3,72}$. We used fmincon in MATLAB with a least squares formulation to estimate M_1, M_2 and M_3 based on these constraints. We repeated this estimation 5 times with random initial guesses, each converging to the same values, demonstrating uniqueness of the estimates. The best fit values are given in Table 1 below.

Drug dose response modeling. Each of the drugs, PD0325901 (MEK1/2 inhibitor—$i = 1$), Abemaciclib (CDK4/6 inhibitor—$i = 2$), and TAK-960 (PLK1 inhibitor—$i = 3$), were modeled as having an inhibitory effect on the respective Markov parameters M_1, M_2 and M_3. We used a sigmoidal hill-type function to describe the effect of drug concentration on transition rates as follows

$$M_i = M_{io} \times \left(1 - \frac{(D_i/EC_{50i})^{n_i}}{1 + (D_i/EC_{50i})^{n_i}}\right) \tag{6}$$

where M_{io} is the best fit transition parameter from above, D_i is drug dose, and unknown parameters are EC_{50i} and n_i.

To model the effect of drug on cell death and account for data at high drug doses, we added the following term to the model

$$M_{i,\varphi} = \frac{E_{maxi,\varphi}(D_i/EC_{50i,\varphi})}{1 + (D_i/EC_{50i,\varphi})} \tag{7}$$

where, $E_{maxi,\varphi}$ and $EC_{50i,\varphi}$ are parameters to be estimated as above, with Eq 5 changing as follows:

$$x_{i,t+1} = (1 - M_i - M_{i,\varphi})x_{i,t} + f \times M_j x_{j,t}$$

$$if \; i = 1 : f = 2, j = 3$$

$$if \; i = 2,3 : f = 1, j = i - 1 \tag{8}$$

We used lsqnonlin in MATLAB to estimate these unknown parameters by minimizing the sum of squared errors between model predicted and measured relative cell counts at 72 hours post drug treatment. The best fit parameters are summarized in Table 2 below. AIC calculations for cases of death (24 free parameters) or no death terms (12 free parameters) assumed standard normal distributed errors (residuals normalized by experimental standard deviation). We used normpdf in MATLAB to calculate likelihood function contributions.

Excess over Bliss analysis.   We used a robust excess over Bliss (EOB) [73] as the basis for these calculations. Consider each row in the combination drug dose response matrix. One of the drug's doses would be constant across the row but the dose of the other drug increases from left to right. This can be captured by a 4-parameter logistic model [73,117]-

$$y = \frac{E_{min} + E_{max}(D/EC_{50})^n}{1 + (D/EC_{50})^n} \tag{9}$$

where y is the inhibition effect (1—the measured relative cell number), E_{min} is the minimal possible inhibition effect, E_{max} is the maximum possible inhibition effect, EC_{50} is the half maximal parameter and n is the Hill coefficient.

We used `lsqcurvefit` in MATLAB to obtain least-squares estimates for the four-parameters for each of the 8 rows and 8 columns. For a particular drug combination point, the average of the two fitted inhibition values from its row and column estimates was taken as the final fitted inhibition value (y_{AB}). Consider the fitted inhibition values for particular doses of drug A alone (y_A), drug B alone (y_B) and their combination (y_{AB}). The Bliss independence scores [33,72,73] are calculated by

$$y_{Bliss,AB} = y_A + y_B - y_A y_B \tag{10}$$

and the *EOB* scores are calculated by

$$EOB_{AB} = y_{AB} - y_{Bliss,AB}. \tag{11}$$

These scores evaluated at each dose combination are averaged across the dataset for a single EOB score for each drug combination / cell line pair.

Supporting information

S1 Code. This file contains all the MATLAB code necessary to reproduce the figures and analyses in the manuscript (see also Methods).
(ZIP)

S1 Text. Which contains the following Figures: Fig A. Single Drug Dose Response Fits for a Model with No Drug-Induced Cell Death. The model was fit as described in Methods, but there was no ability for drugs to influence cell death. This model could not account for much of the drug action at high concentrations. **Fig B. Goodness-of-Fit for Single Drug Dose Responses.** For each fit shown in Fig 1D, relative cell number for model simulations was plotted vs experimental data. The correlation coefficient was calculated and is shown within each plot. **Fig C. Goodness-of-Fit for Drug Combination Responses for Varying Ranges of Doubling Time and Cell State Ratios.** The doubling times and cell state ratios for cell lines can vary from lab-to-lab, and we used reported ranges for U87 and U251 cells to perform drug combination response simulations as in the manuscript. The correlation between model simulations and experimental data for drug combination responses is shown, and variation in these parameters has minimal effect. Error bars denote standard error. Correlation coefficients are shown in each plot.
(DOCX)

Author Contributions

Conceptualization: Deepraj Sarmah, Marc R. Birtwistle.

Data curation: Deepraj Sarmah.

Formal analysis: Deepraj Sarmah, Marc R. Birtwistle.

Investigation: Deepraj Sarmah, Wesley O. Meredith, Ian K. Weber, Madison R. Price.

Supervision: Marc R. Birtwistle.

Validation: Deepraj Sarmah.

Visualization: Deepraj Sarmah, Marc R. Birtwistle.

Writing – original draft: Deepraj Sarmah, Marc R. Birtwistle.

Writing – review & editing: Deepraj Sarmah, Marc R. Birtwistle.

References

1. Chapman PB, Hauschild A, Robert C, Haanen JB, Ascierto P, Larkin J, et al. Improved Survival with Vemurafenib in Melanoma with BRAF V600E Mutation. New England Journal of Medicine. 2011; 364: 2507–2516. https://doi.org/10.1056/NEJMoa1103782 PMID: 21639808

2. Sosman JA, Kim KB, Schuchter L, Gonzalez R, Pavlick AC, Weber JS, et al. Survival in BRAF V600–Mutant Advanced Melanoma Treated with Vemurafenib. New England Journal of Medicine. 2012; 366: 707–714. https://doi.org/10.1056/NEJMoa1112302 PMID: 22356324

3. Herbst RS, Fukuoka M, Baselga J. Gefitinib—a novel targeted approach to treating cancer. Nat Rev Cancer. 2004; 4: 956–965. https://doi.org/10.1038/nrc1506 PMID: 15573117

4. Paez JG, Jänne PA, Lee JC, Tracy S, Greulich H, Gabriel S, et al. EGFR Mutations in Lung Cancer: Correlation with Clinical Response to Gefitinib Therapy. Science. 2004; 304: 1497–1500. https://doi.org/10.1126/science.1099314 PMID: 15118125

5. Takano T, Ohe Y, Sakamoto H, Tsuta K, Matsuno Y, Tateishi U, et al. Epidermal Growth Factor Receptor Gene Mutations and Increased Copy Numbers Predict Gefitinib Sensitivity in Patients With Recurrent Non–Small-Cell Lung Cancer. JCO. 2005; 23: 6829–6837. https://doi.org/10.1200/JCO.2005.01.0793 PMID: 15998907

6. Druker BJ, Lydon NB. Lessons learned from the development of an Abl tyrosine kinase inhibitor for chronic myelogenous leukemia. J Clin Invest. 2000; 105: 3–7. https://doi.org/10.1172/JCI9083 PMID: 10619854

7. Druker BJ, Guilhot F, O'Brien SG, Gathmann I, Kantarjian H, Gattermann N, et al. Five-Year Follow-up of Patients Receiving Imatinib for Chronic Myeloid Leukemia. New England Journal of Medicine. 2006; 355: 2408–2417. https://doi.org/10.1056/NEJMoa062867 PMID: 17151364

8. Hudis CA. Trastuzumab—Mechanism of Action and Use in Clinical Practice. New England Journal of Medicine. 2007; 357: 39–51. https://doi.org/10.1056/NEJMra043186 PMID: 17611206

9. Slamon D, Eiermann W, Robert N, Pienkowski T, Martin M, Press M, et al. Adjuvant Trastuzumab in HER2-Positive Breast Cancer. New England Journal of Medicine. 2011; 365: 1273–1283. https://doi.org/10.1056/NEJMoa0910383 PMID: 21991949

10. Landau DA, Carter SL, Stojanov P, McKenna A, Stevenson K, Lawrence MS, et al. Evolution and impact of subclonal mutations in chronic lymphocytic leukemia. Cell. 2013; 152: 714–26. https://doi.org/10.1016/j.cell.2013.01.019 PMID: 23415222

11. Bailey P, Chang DK, Nones K, Johns AL, Patch A-M, Gingras M-C, et al. Genomic analyses identify molecular subtypes of pancreatic cancer. Nature. 2016; 531: 47–52. https://doi.org/10.1038/nature16965 PMID: 26909576

12. Guinney J, Dienstmann R, Wang X, de Reyniès A, Schlicker A, Soneson C, et al. The consensus molecular subtypes of colorectal cancer. Nat Med. 2015; 21: 1350–1356. https://doi.org/10.1038/nm.3967 PMID: 26457759

13. Neftel C, Laffy J, Filbin MG, Hara T, Shore ME, Rahme GJ, et al. An Integrative Model of Cellular States, Plasticity, and Genetics for Glioblastoma. Cell. 2019; 178: 835–849.e21. https://doi.org/10.1016/j.cell.2019.06.024 PMID: 31327527

14. Rudin CM, Poirier JT, Byers LA, Dive C, Dowlati A, George J, et al. Molecular subtypes of small cell lung cancer: a synthesis of human and mouse model data. Nat Rev Cancer. 2019; 19: 289–297. https://doi.org/10.1038/s41568-019-0133-9 PMID: 30926931

15. Wang Q, Hu B, Hu X, Kim H, Squatrito M, Scarpace L, et al. Tumor Evolution of Glioma-Intrinsic Gene Expression Subtypes Associates with Immunological Changes in the Microenvironment. Cancer Cell. 2017; 32: 42–56.e6. https://doi.org/10.1016/j.ccell.2017.06.003 PMID: 28697342

16. Yersal O, Barutca S. Biological subtypes of breast cancer: Prognostic and therapeutic implications. World Journal of Clinical Oncology. 2014; 5: 412–424. https://doi.org/10.5306/wjco.v5.i3.412 PMID: 25114856

17. Rukhlenko OS, Halasz M, Rauch N, Zhernovkov V, Prince T, Wynne K, et al. Control of cell state transitions. Nature. 2022; 609: 975–985. https://doi.org/10.1038/s41586-022-05194-y PMID: 36104561

18. Gupta PB, Fillmore CM, Jiang G, Shapira SD, Tao K, Kuperwasser C, et al. Stochastic State Transitions Give Rise to Phenotypic Equilibrium in Populations of Cancer Cells. Cell. 2011; 146: 633–644. https://doi.org/10.1016/j.cell.2011.07.026 PMID: 21854987

19. Boumahdi S, de Sauvage FJ. The great escape: tumour cell plasticity in resistance to targeted therapy. Nat Rev Drug Discov. 2020; 19: 39–56. https://doi.org/10.1038/s41573-019-0044-1 PMID: 31601994

20. Brown R, Curry E, Magnani L, Wilhelm-Benartzi CS, Borley J. Poised epigenetic states and acquired drug resistance in cancer. Nat Rev Cancer. 2014; 14: 747–753. https://doi.org/10.1038/nrc3819 PMID: 25253389

21. Easwaran H, Tsai H-C, Baylin SB. Cancer Epigenetics: Tumor Heterogeneity, Plasticity of Stem-like States, and Drug Resistance. Molecular Cell. 2014; 54: 716–727. https://doi.org/10.1016/j.molcel.2014.05.015 PMID: 24905005

22. Csermely P, Korcsmáros T, Kiss HJM, London G, Nussinov R. Structure and dynamics of molecular networks: A novel paradigm of drug discovery: A comprehensive review. Pharmacology & Therapeutics. 2013; 138: 333–408. https://doi.org/10.1016/j.pharmthera.2013.01.016 PMID: 23384594

23. Hornberg JJ, Bruggeman FJ, Westerhoff HV, Lankelma J. Cancer: A Systems Biology disease. Biosystems. 2006; 83: 81–90. https://doi.org/10.1016/j.biosystems.2005.05.014 PMID: 16426740

24. Kolch W, Pitt A. Functional proteomics to dissect tyrosine kinase signalling pathways in cancer. Nat Rev Cancer. 2010; 10: 618–629. https://doi.org/10.1038/nrc2900 PMID: 20720570

25. Krogan NJ, Lippman S, Agard DA, Ashworth A, Ideker T. The Cancer Cell Map Initiative: Defining the Hallmark Networks of Cancer. Molecular Cell. 2015; 58: 690–698. https://doi.org/10.1016/j.molcel.2015.05.008 PMID: 26000852

26. Moustakas A, Heldin C-H. Signaling networks guiding epithelial–mesenchymal transitions during embryogenesis and cancer progression. Cancer Science. 2007; 98: 1512–1520. https://doi.org/10.1111/j.1349-7006.2007.00550.x PMID: 17645776

27. Yin N, Ma W, Pei J, Ouyang Q, Tang C, Lai L. Synergistic and antagonistic drug combinations depend on network topology. PLoS One. 2014; 9: e93960. https://doi.org/10.1371/journal.pone.0093960 PMID: 24713621

28. Flaherty KT, Infante JR, Daud A, Gonzalez R, Kefford RF, Sosman J, et al. Combined BRAF and MEK Inhibition in Melanoma with BRAF V600 Mutations. New England Journal of Medicine. 2012; 367: 1694–1703. https://doi.org/10.1056/NEJMoa1210093 PMID: 23020132

29. Long GV, Stroyakovskiy D, Gogas H, Levchenko E, de Braud F, Larkin J, et al. Combined BRAF and MEK Inhibition versus BRAF Inhibition Alone in Melanoma. New England Journal of Medicine. 2014; 371: 1877–1888. https://doi.org/10.1056/NEJMoa1406037 PMID: 25265492

30. Poulikakos PI, Zhang C, Bollag G, Shokat KM, Rosen N. RAF inhibitors transactivate RAF dimers and ERK signalling in cells with wild-type BRAF. Nature. 2010; 464: 427–430. https://doi.org/10.1038/nature08902 PMID: 20179705

31. Rukhlenko OS, Khorsand F, Krstic A, Rozanc J, Alexopoulos LG, Rauch N, et al. Dissecting RAF Inhibitor Resistance by Structure-based Modeling Reveals Ways to Overcome Oncogenic RAS Signaling. Cell Systems. 2018; 7: 161–179.e14. https://doi.org/10.1016/j.cels.2018.06.002 PMID: 30007540

32. Amundson SA, Myers TG, Scudiero D, Kitada S, Reed JC, Fornace AJ Jr. An Informatics Approach Identifying Markers of Chemosensitivity in Human Cancer Cell Lines1. Cancer Research. 2000; 60: 6101–6110.

33. Bansal M, Yang J, Karan C, Menden MP, Costello JC, Tang H, et al. A community computational challenge to predict the activity of pairs of compounds. Nat Biotechnol. 2014; 32: 1213–1222. https://doi.org/10.1038/nbt.3052 PMID: 25419740

34. Barretina J, Caponigro G, Stransky N, Venkatesan K, Margolin AA, Kim S, et al. The Cancer Cell Line Encyclopedia enables predictive modelling of anticancer drug sensitivity. Nature. 2012; 483: 603–607. https://doi.org/10.1038/nature11003 PMID: 22460905

35. Costello JC, Heiser LM, Georgii E, Gönen M, Menden MP, Wang NJ, et al. A community effort to assess and improve drug sensitivity prediction algorithms. Nat Biotechnol. 2014; 32: 1202–1212. https://doi.org/10.1038/nbt.2877 PMID: 24880487

36. Garnett MJ, Edelman EJ, Heidorn SJ, Greenman CD, Dastur A, Lau KW, et al. Systematic identification of genomic markers of drug sensitivity in cancer cells. Nature. 2012; 483: 570–575. https://doi.org/10.1038/nature11005 PMID: 22460902

37. Menden MP, Iorio F, Garnett M, McDermott U, Benes CH, Ballester PJ, et al. Machine Learning Prediction of Cancer Cell Sensitivity to Drugs Based on Genomic and Chemical Properties. PLOS ONE. 2013; 8: e61318. https://doi.org/10.1371/journal.pone.0061318 PMID: 23646105

38. Menden MP, Wang D, Mason MJ, Szalai B, Bulusu KC, Guan Y, et al. Community assessment to advance computational prediction of cancer drug combinations in a pharmacogenomic screen. Nat Commun. 2019; 10: 2674. https://doi.org/10.1038/s41467-019-09799-2 PMID: 31209238

39. Yang W, Soares J, Greninger P, Edelman EJ, Lightfoot H, Forbes S, et al. Genomics of Drug Sensitivity in Cancer (GDSC): a resource for therapeutic biomarker discovery in cancer cells. Nucleic Acids Research. 2013; 41: D955–D961. https://doi.org/10.1093/nar/gks1111 PMID: 23180760

40. Bouhaddou M, Barrette AM, Stern AD, Koch RJ, DiStefano MS, Riesel EA, et al. A mechanistic pan-cancer pathway model informed by multi-omics data interprets stochastic cell fate responses to drugs and mitogens. PLOS Computational Biology. 2018; 14: e1005985. https://doi.org/10.1371/journal.pcbi.1005985 PMID: 29579036

41. Erdem C, Mutsuddy A, Bensman EM, Dodd WB, Saint-Antoine MM, Bouhaddou M, et al. A scalable, open-source implementation of a large-scale mechanistic model for single cell proliferation and death signaling. Nat Commun. 2022; 13: 3555. https://doi.org/10.1038/s41467-022-31138-1 PMID: 35729113

42. Fröhlich F, Kaltenbacher B, Theis FJ, Hasenauer J. Scalable Parameter Estimation for Genome-Scale Biochemical Reaction Networks. PLOS Computational Biology. 2017; 13: e1005331. https://doi.org/10.1371/journal.pcbi.1005331 PMID: 28114351

43. Li J, Xu H, McIndoe RA. A novel network based linear model for prioritization of synergistic drug combinations. PLOS ONE. 2022; 17: e0266382. https://doi.org/10.1371/journal.pone.0266382 PMID: 35381038

44. Narayan RS, Molenaar P, Teng J, Cornelissen FMG, Roelofs I, Menezes R, et al. A cancer drug atlas enables synergistic targeting of independent drug vulnerabilities. Nat Commun. 2020; 11: 2935. https://doi.org/10.1038/s41467-020-16735-2 PMID: 32523045

45. Vamathevan J, Clark D, Czodrowski P, Dunham I, Ferran E, Lee G, et al. Applications of machine learning in drug discovery and development. Nat Rev Drug Discov. 2019; 18: 463–477. https://doi.org/10.1038/s41573-019-0024-5 PMID: 30976107

46. Chen D, Liu X, Yang Y, Yang H, Lu P. Systematic synergy modeling: understanding drug synergy from a systems biology perspective. BMC Syst Biol. 2015; 9: 56. https://doi.org/10.1186/s12918-015-0202-y PMID: 26377814

47. Cheng F, Kovács IA, Barabási A-L. Network-based prediction of drug combinations. Nat Commun. 2019; 10: 1197. https://doi.org/10.1038/s41467-019-09186-x PMID: 30867426

48. Tang J, Gautam P, Gupta A, He L, Timonen S, Akimov Y, et al. Network pharmacology modeling identifies synergistic Aurora B and ZAK interaction in triple-negative breast cancer. npj Syst Biol Appl. 2019; 5: 1–11. https://doi.org/10.1038/s41540-019-0098-z PMID: 31312514

49. Tai Y-T, Kim K, Li X-F, Fulciniti M, Song W, Nahar S, et al. Targeting MEK1/2 Signaling Cascade by AS703026, a Novel Selective MEK1/2 Inhibitor, Induces Pleiotropic Anti-Myeloma Activity in Vitro and In Vivo. Blood. 2009; 114: 3848. https://doi.org/10.1182/blood.V114.22.3848.3848

50. Burkhart DL, Sage J. Cellular mechanisms of tumour suppression by the retinoblastoma gene. Nat Rev Cancer. 2008; 8: 671–682. https://doi.org/10.1038/nrc2399 PMID: 18650841

51. Kent LN, Leone G. The broken cycle: E2F dysfunction in cancer. Nat Rev Cancer. 2019; 19: 326–338. https://doi.org/10.1038/s41568-019-0143-7 PMID: 31053804

52. Malumbres M, Barbacid M. Cell cycle, CDKs and cancer: a changing paradigm. Nat Rev Cancer. 2009; 9: 153–166. https://doi.org/10.1038/nrc2602 PMID: 19238148

53. Otto T, Sicinski P. Cell cycle proteins as promising targets in cancer therapy. Nat Rev Cancer. 2017; 17: 93–115. https://doi.org/10.1038/nrc.2016.138 PMID: 28127048

54. Gheghiani L, Loew D, Lombard B, Mansfeld J, Gavet O. PLK1 Activation in Late G2 Sets Up Commitment to Mitosis. Cell Reports. 2017; 19: 2060–2073. https://doi.org/10.1016/j.celrep.2017.05.031 PMID: 28591578

55. Lan R, Lin G, Yin F, Xu J, Zhang X, Wang J, et al. Dissecting the phenotypes of Plk1 inhibition in cancer cells using novel kinase inhibitory chemical CBB2001. Lab Invest. 2012; 92: 1503–1514. https://doi.org/10.1038/labinvest.2012.114 PMID: 22890557

56. Pezuk JA, Brassesco MS, Morales AG, de Oliveira JC, de Oliveira HF, Scrideli CA, et al. Inhibition of Polo-Like Kinase 1 Induces Cell Cycle Arrest and Sensitizes Glioblastoma Cells to Ionizing Radiation.

Cancer Biother Radiopharm. 2013; 28: 516–522. https://doi.org/10.1089/cbr.2012.1415 PMID: 23713868

57. Zhang Z, Su W-H, Feng C, Yu D-H, Cui C, Xu X-Y, et al. Polo-like kinase 1 may regulate G2/M transition of mouse fertilized eggs by means of inhibiting the phosphorylation of Tyr 15 of Cdc2. Mol Reprod Dev. 2007; 74: 1247–1254. https://doi.org/10.1002/mrd.20703 PMID: 17342725

58. Jin S-G, Ryu H-H, Li S-Y, Li C-H, Lim S-H, Jang W-Y, et al. Nogo-A inhibits the migration and invasion of human malignant glioma U87MG cells. Oncology Reports. 2016; 35: 3395–3402. https://doi.org/10.3892/or.2016.4737 PMID: 27109183

59. Lane R, Simon T, Vintu M, Solkin B, Koch B, Stewart N, et al. Cell-derived extracellular vesicles can be used as a biomarker reservoir for glioblastoma tumor subtyping. Commun Biol. 2019; 2: 1–12. https://doi.org/10.1038/s42003-019-0560-x PMID: 31453379

60. Oraiopoulou M-E, Tzamali E, Tzedakis G, Vakis A, Papamatheakis J, Sakkalis V. In Vitro/In Silico Study on the Role of Doubling Time Heterogeneity among Primary Glioblastoma Cell Lines. BioMed Research International. 2017; 2017: e8569328. https://doi.org/10.1155/2017/8569328 PMID: 29226151

61. Cowley GS, Weir BA, Vazquez F, Tamayo P, Scott JA, Rusin S, et al. Parallel genome-scale loss of function screens in 216 cancer cell lines for the identification of context-specific genetic dependencies. Sci Data. 2014; 1: 140035. https://doi.org/10.1038/sdata.2014.35 PMID: 25984343

62. Lee DW, Lee M-Y, Ku B, Nam D-H. Automatic 3D Cell Analysis in High-Throughput Microarray Using Micropillar and Microwell Chips. J Biomol Screen. 2015; 20: 1178–1184. https://doi.org/10.1177/1087057115597635 PMID: 26239238

63. Weller M, Rieger J, Grimmel C, Van Meir EG, De Tribolet N, Krajewski S, et al. Predicting chemoresistance in human malignant glioma cells: The role of molecular genetic analyses. International Journal of Cancer. 1998; 79: 640–644. https://doi.org/10.1002/(sici)1097-0215(19981218)79:6<640::aid-ijc15>3.0.co;2-z PMID: 9842975

64. Anandharaj A, Cinghu S, Park W-Y. Rapamycin-mediated mTOR inhibition attenuates survivin and sensitizes glioblastoma cells to radiation therapy. Acta Biochimica et Biophysica Sinica. 2011; 43: 292–300. https://doi.org/10.1093/abbs/gmr012 PMID: 21367753

65. Hu G, Cun X, Ruan S, Shi K, Wang Y, Kuang Q, et al. Utilizing G2/M retention effect to enhance tumor accumulation of active targeting nanoparticles. Sci Rep. 2016; 6: 27669. https://doi.org/10.1038/srep27669 PMID: 27273770

66. Pisapia L, Barba P, Cortese A, Cicatiello V, Morelli F, Del Pozzo G. EBP1 protein modulates the expression of human MHC class II molecules in non-hematopoietic cancer cells. International Journal of Oncology. 2015; 47: 481–489. https://doi.org/10.3892/ijo.2015.3051 PMID: 26081906

67. Metabolic Impact of Anti-Angiogenic Agents on U87 Glioma Cells. PLOS ONE. 2014; 9: e99198. https://doi.org/10.1371/journal.pone.0099198 PMID: 24922514

68. Xu P-F, Yang J-A, Liu J-H, Yang X, Liao J-M, Yuan F-E, et al. PI3Kβ inhibitor AZD6482 exerts antiproliferative activity and induces apoptosis in human glioblastoma cells. Oncol Rep. 2019; 41: 125–132. https://doi.org/10.3892/or.2018.6845 PMID: 30542720

69. He X, Maimaiti M, Jiao Y, Meng X, Li H. Sinomenine Induces G1-Phase Cell Cycle Arrest and Apoptosis in Malignant Glioma Cells Via Downregulation of Sirtuin 1 and Induction of p53 Acetylation. Technol Cancer Res Treat. 2018; 17: 1533034618770305. https://doi.org/10.1177/1533034618770305 PMID: 29756546

70. Liu Y, Wang F, Liu Y, Yao Y, Lv X, Dong B, et al. RNF135, RING finger protein, promotes the proliferation of human glioblastoma cells in vivo and in vitro via the ERK pathway. Sci Rep. 2016; 6: 20642. https://doi.org/10.1038/srep20642 PMID: 26856755

71. ZHANG Y, CHEN X, LIAN H, LIU J, ZHOU B, HAN S, et al. MicroRNA-503 acts as a tumor suppressor in glioblastoma for multiple antitumor effects by targeting IGF-1R. Oncol Rep. 2014; 31: 1445–1452. https://doi.org/10.3892/or.2013.2951 PMID: 24378652

72. Bliss CI. THE CALCULATION OF MICROBIAL ASSAYS. Bacteriol Rev. 1956; 20: 243–258. https://doi.org/10.1128/br.20.4.243-258.1956 PMID: 13403845

73. Yadav B, Wennerberg K, Aittokallio T, Tang J. Searching for Drug Synergy in Complex Dose–Response Landscapes Using an Interaction Potency Model. Comput Struct Biotechnol J. 2015; 13: 504–513. https://doi.org/10.1016/j.csbj.2015.09.001 PMID: 26949479

74. Holbeck SL, Camalier R, Crowell JA, Govindharajulu JP, Hollingshead M, Anderson LW, et al. The National Cancer Institute ALMANAC: A Comprehensive Screening Resource for the Detection of Anticancer Drug Pairs with Enhanced Therapeutic Activity. Cancer Research. 2017; 77: 3564–3576. https://doi.org/10.1158/0008-5472.CAN-17-0489 PMID: 28446463

75. O'Neil J, Benita Y, Feldman I, Chenard M, Roberts B, Liu Y, et al. An Unbiased Oncology Compound Screen to Identify Novel Combination Strategies. Molecular Cancer Therapeutics. 2016; 15: 1155–1162. https://doi.org/10.1158/1535-7163.MCT-15-0843 PMID: 26983881

76. Lee MS, Helms TL, Feng N, Gay J, Chang QE, Tian F, et al. Efficacy of the combination of MEK and CDK4/6 inhibitors in vitro and in vivo in KRAS mutant colorectal cancer models. Oncotarget. 2016; 7: 39595–39608. https://doi.org/10.18632/oncotarget.9153 PMID: 27167191

77. Franco J, Witkiewicz AK, Knudsen ES. CDK4/6 inhibitors have potent activity in combination with pathway selective therapeutic agents in models of pancreatic cancer. Oncotarget. 2014; 5: 6512–6525. https://doi.org/10.18632/oncotarget.2270 PMID: 25156567

78. de Leeuw R, McNair C, Schiewer MJ, Neupane NP, Brand LJ, Augello MA, et al. MAPK Reliance via Acquired CDK4/6 Inhibitor Resistance in Cancer. Clinical Cancer Research. 2018; 24: 4201–4214. https://doi.org/10.1158/1078-0432.CCR-18-0410 PMID: 29739788

79. Forschner A, Sinnberg T, Mroz G, Schroeder C, Reinert CP, Gatidis S, et al. Case Report: Combined CDK4/6 and MEK Inhibition in Refractory CDKN2A and NRAS Mutant Melanoma. Front Oncol. 2021; 11: 643156. https://doi.org/10.3389/fonc.2021.643156 PMID: 33732653

80. Margue C, Philippidou D, Kozar I, Cesi G, Felten P, Kulms D, et al. Kinase inhibitor library screening identifies synergistic drug combinations effective in sensitive and resistant melanoma cells. J Exp Clin Cancer Res. 2019; 38: 56. https://doi.org/10.1186/s13046-019-1038-x PMID: 30728057

81. Posch C, Cholewa BD, Vujic I, Sanlorenzo M, Ma J, Kim ST, et al. Combined Inhibition of MEK and Plk1 Has Synergistic Antitumor Activity in NRAS Mutant Melanoma. Journal of Investigative Dermatology. 2015; 135: 2475–2483. https://doi.org/10.1038/jid.2015.198 PMID: 26016894

82. Montaudon E, Nikitorowicz-Buniak J, Sourd L, Morisset L, El Botty R, Huguet L, et al. PLK1 inhibition exhibits strong anti-tumoral activity in CCND1-driven breast cancer metastases with acquired palbociclib resistance. Nat Commun. 2020; 11: 4053. https://doi.org/10.1038/s41467-020-17697-1 PMID: 32792481

83. Schmucker R, Farina G, Faeder J, Fröhlich F, Saglam AS, Sandholm T. Combination treatment optimization using a pan-cancer pathway model. Scott JG, editor. PLoS Comput Biol. 2021; 17: e1009689. https://doi.org/10.1371/journal.pcbi.1009689 PMID: 34962919

84. Poleszczuk J, Macklin P, Enderling H. Agent-Based Modeling of Cancer Stem Cell Driven Solid Tumor Growth. In: Turksen K, editor. Stem Cell Heterogeneity. New York, NY: Springer New York; 2016. pp. 335–346. https://doi.org/10.1007/7651_2016_346 PMID: 27044046

85. Gong C, Milberg O, Wang B, Vicini P, Narwal R, Roskos L, et al. A computational multiscale agent-based model for simulating spatio-temporal tumour immune response to PD1 and PDL1 inhibition. J R Soc Interface. 2017; 14: 20170320. https://doi.org/10.1098/rsif.2017.0320 PMID: 28931635

86. Letort G, Montagud A, Stoll G, Heiland R, Barillot E, Macklin P, et al. PhysiBoSS: a multi-scale agent-based modelling framework integrating physical dimension and cell signalling. Wren J, editor. Bioinformatics. 2019; 35: 1188–1196. https://doi.org/10.1093/bioinformatics/bty766 PMID: 30169736

87. Bravo RR, Baratchart E, West J, Schenck RO, Miller AK, Gallaher J, et al. Hybrid Automata Library: A flexible platform for hybrid modeling with real-time visualization. Merks RMH, editor. PLoS Comput Biol. 2020; 16: e1007635. https://doi.org/10.1371/journal.pcbi.1007635 PMID: 32155140

88. Ghaffarizadeh A, Heiland R, Friedman SH, Mumenthaler SM, Macklin P. PhysiCell: An open source physics-based cell simulator for 3-D multicellular systems. Poisot T, editor. PLoS Comput Biol. 2018; 14: e1005991. https://doi.org/10.1371/journal.pcbi.1005991 PMID: 29474446

89. Basanta D, Gatenby RA, Anderson ARA. Exploiting evolution to treat drug resistance: combination therapy and the double bind. Mol Pharm. 2012; 9: 914–921. https://doi.org/10.1021/mp200458e PMID: 22369188

90. Zhang J, Cunningham JJ, Brown JS, Gatenby RA. Integrating evolutionary dynamics into treatment of metastatic castrate-resistant prostate cancer. Nat Commun. 2017; 8: 1816. https://doi.org/10.1038/s41467-017-01968-5 PMID: 29180633

91. Strobl MAR, Gallaher J, West J, Robertson-Tessi M, Maini PK, Anderson ARA. Spatial structure impacts adaptive therapy by shaping intra-tumoral competition. Commun Med. 2022; 2: 46. https://doi.org/10.1038/s43856-022-00110-x PMID: 35603284

92. West J, You L, Zhang J, Gatenby RA, Brown JS, Newton PK, et al. Towards Multidrug Adaptive Therapy. Cancer Research. 2020; 80: 1578–1589. https://doi.org/10.1158/0008-5472.CAN-19-2669 PMID: 31948939

93. Silva AS, Gatenby RA. A theoretical quantitative model for evolution of cancer chemotherapy resistance. Biol Direct. 2010; 5: 25. https://doi.org/10.1186/1745-6150-5-25 PMID: 20406443

94. Liu H, Zhang W, Zou B, Wang J, Deng Y, Deng L. DrugCombDB: a comprehensive database of drug combinations toward the discovery of combinatorial therapy. Nucleic Acids Research. 2020; 48: D871–D881. https://doi.org/10.1093/nar/gkz1007 PMID: 31665429

95. Shtar G, Azulay L, Nizri O, Rokach L, Shapira B. CDCDB: A large and continuously updated drug combination database. Sci Data. 2022; 9: 263. https://doi.org/10.1038/s41597-022-01360-z PMID: 35654801

96. Patel AP, Tirosh I, Trombetta JJ, Shalek AK, Gillespie SM, Wakimoto H, et al. Single-cell RNA-seq highlights intratumoral heterogeneity in primary glioblastoma. Science. 2014; 344: 1396–1401. https://doi.org/10.1126/science.1254257 PMID: 24925914

97. Bhowmick NA, Ghiassi M, Bakin A, Aakre M, Lundquist CA, Engel ME, et al. Transforming Growth Factor-β1 Mediates Epithelial to Mesenchymal Transdifferentiation through a RhoA-dependent Mechanism. MBoC. 2001; 12: 27–36. https://doi.org/10.1091/mbc.12.1.27 PMID: 11160820

98. Bolós V, Peinado H, Pérez-Moreno MA, Fraga MF, Esteller M, Cano A. The transcription factor Slug represses E-cadherin expression and induces epithelial to mesenchymal transitions: a comparison with Snail and E47 repressors. Journal of Cell Science. 2003; 116: 499–511. https://doi.org/10.1242/jcs.00224 PMID: 12508111

99. Tania M, Khan MdA, Fu J. Epithelial to mesenchymal transition inducing transcription factors and metastatic cancer. Tumor Biol. 2014; 35: 7335–7342. https://doi.org/10.1007/s13277-014-2163-y PMID: 24880591

100. Schlauch D, Glass K, Hersh CP, Silverman EK, Quackenbush J. Estimating drivers of cell state transitions using gene regulatory network models. BMC Systems Biology. 2017; 11: 139. https://doi.org/10.1186/s12918-017-0517-y PMID: 29237467

101. Sehl ME, Shimada M, Landeros A, Lange K, Wicha MS. Modeling of Cancer Stem Cell State Transitions Predicts Therapeutic Response. PLOS ONE. 2015; 10: e0135797. https://doi.org/10.1371/journal.pone.0135797 PMID: 26397099

102. Su Y, Wei W, Robert L, Xue M, Tsoi J, Garcia-Diaz A, et al. Single-cell analysis resolves the cell state transition and signaling dynamics associated with melanoma drug-induced resistance. Proceedings of the National Academy of Sciences. 2017; 114: 13679–13684. https://doi.org/10.1073/pnas.1712064115 PMID: 29229836

103. Kholodenko BN, Kiyatkin A, Bruggeman FJ, Sontag E, Westerhoff HV, Hoek JB. Untangling the wires: A strategy to trace functional interactions in signaling and gene networks. Proceedings of the National Academy of Sciences. 2002; 99: 12841–12846. https://doi.org/10.1073/pnas.192442699 PMID: 12242336

104. Lill D, Rukhlenko OS, Mc Elwee AJ, Kashdan E, Timmer J, Kholodenko BN. Mapping connections in signaling networks with ambiguous modularity. npj Syst Biol Appl. 2019; 5: 1–11. https://doi.org/10.1038/s41540-019-0096-1 PMID: 31149348

105. Sontag E, Kiyatkin A, Kholodenko BN. Inferring dynamic architecture of cellular networks using time series of gene expression, protein and metabolite data. Bioinformatics. 2004; 20: 1877–1886. https://doi.org/10.1093/bioinformatics/bth173 PMID: 15037511

106. Thomaseth C, Fey D, Santra T, Rukhlenko OS, Radde NE, Kholodenko BN. Impact of measurement noise, experimental design, and estimation methods on Modular Response Analysis based network reconstruction. Sci Rep. 2018; 8: 16217. https://doi.org/10.1038/s41598-018-34353-3 PMID: 30385767

107. Sarmah D, Smith GR, Bouhaddou M, Stern AD, Erskine J, Birtwistle MR. Network inference from perturbation time course data. NPJ Syst Biol Appl. 2022; 8: 42. https://doi.org/10.1038/s41540-022-00253-6 PMID: 36316338

108. Armond JW, Saha K, Rana AA, Oates CJ, Jaenisch R, Nicodemi M, et al. A stochastic model dissects cell states in biological transition processes. Sci Rep. 2014; 4: 3692. https://doi.org/10.1038/srep03692 PMID: 24435049

109. Buder T, Deutsch A, Seifert M, Voss-Böhme A. CellTrans: An R Package to Quantify Stochastic Cell State Transitions. Bioinform Biol Insights. 2017; 11: 1177932217712241. https://doi.org/10.1177/1177932217712241 PMID: 28659714

110. Jagannathan NS, Ihsan MO, Kin XX, Welsch RE, Clément M-V, Tucker-Kellogg L. Transcompp: understanding phenotypic plasticity by estimating Markov transition rates for cell state transitions. Bioinformatics. 2020; 36: 2813–2820. https://doi.org/10.1093/bioinformatics/btaa021 PMID: 31971581

111. Sáez M, Blassberg R, Camacho-Aguilar E, Siggia ED, Rand DA, Briscoe J. Statistically derived geometrical landscapes capture principles of decision-making dynamics during cell fate transitions. Cell Systems. 2022; 13: 12–28.e3. https://doi.org/10.1016/j.cels.2021.08.013 PMID: 34536382

112. Stumpf PS, Smith RCG, Lenz M, Schuppert A, Müller F-J, Babtie A, et al. Stem Cell Differentiation as a Non-Markov Stochastic Process. Cell Systems. 2017; 5: 268–282.e7. https://doi.org/10.1016/j.cels.2017.08.009 PMID: 28957659

113. Wang S-W, Herriges MJ, Hurley K, Kotton DN, Klein AM. CoSpar identifies early cell fate biases from single-cell transcriptomic and lineage information. Nat Biotechnol. 2022; 40: 1066–1074. https://doi.org/10.1038/s41587-022-01209-1 PMID: 35190690

114. Zhou P, Wang S, Li T, Nie Q. Dissecting transition cells from single-cell transcriptome data through multiscale stochastic dynamics. Nat Commun. 2021; 12: 5609. https://doi.org/10.1038/s41467-021-25548-w PMID: 34556644

115. Weinreb C, Rodriguez-Fraticelli A, Camargo FD, Klein AM. Lineage tracing on transcriptional landscapes links state to fate during differentiation. Science. 2020; 367: eaaw3381. https://doi.org/10.1126/science.aaw3381 PMID: 31974159

116. Mulas C, Chaigne A, Smith A, Chalut KJ. Cell state transitions: definitions and challenges. Development. 2021; 148: dev199950. https://doi.org/10.1242/dev.199950 PMID: 34932803

117. Prinz H. Hill coefficients, dose–response curves and allosteric mechanisms. J Chem Biol. 2009; 3: 37–44. https://doi.org/10.1007/s12154-009-0029-3 PMID: 19779939